Review

JOURNAL OF ADVANCED DIELECTRICS
Vol. 3, No. 1 (2013) 1330001 (14 pages)

DOI: 10.1142/S2010135X13300016

World Scientific
www.worldscientific.com

A review on the dielectric materials for high energy-storage application

Xihong Hao
Laboratory of Integrated Exploitation of Bayan Obo Multi-Metal Resources Inner Mongolia University of Science and Technology, Baotou 014010, P. R. China
and
School of Materials and Metallurgy Inner Mongolia University of Science and Technology, Baotou 014010, P. R. China
xhhao@imust.en

Received 5 February 2013; Revised 1 March 2013; Accepted 3 March 2013; Published 8 April 2013

With the fast development of the power electronics, dielectric materials with high energy-storage density, low loss, and good temperature stability are eagerly desired for the potential application in advanced pulsed capacitors. Based on the physical principals, the materials with higher saturated polarization, smaller remnant polarization, and higher electrical breakdown field are the most promising candidates. According to this rule, so far, four kinds of materials, namely antiferroelectrics, dielectric glass-ceramics, relaxor ferroelectric and polymer-based ferroelectrics are thought to be more likely used in next-generation pulsed capacitors, and have been widely studied. Thus, this review serves to give an overall summary on the state-of-the-art progress on electric energy-storage performance in these materials. Moreover, some general future prospects are also provided from the existed theoretical and experimental results in this work, in order to propel their application in practice.

Keywords: Microstructure; energy storage; dielectric properties; antiferroelectrics; glass-ceramic; relaxor ferroelectrics; polymers.

1. Introduction

Because of the global air pollution, energy deficiency and climate change, various new energy generation technologies, such as solar, wind and thermal energy, are developed to replace the fossil fuel energy resources with cleaner renewable sources. It in turn leads to the high demand of the devices for effectively storing, absorbing, and supplying the electricity. According to the energy-storage time, the commercial devices for electric energy storage are generally divided into two classes: short term and long term. Usually, battery is the long-term one, capacitor is the short-term one. Batteries possess high energy-density (10−300 W·h/kg), but their power density is quite low (typically lower than 500 W/kg) because of the slow movement of the charge carriers, which are mainly used for the long-term and stable energy supply.[1] Differently, capacitors usually have high power density ($10^1 - 10^6$ W/kg for electrochemical supercapacitor and up to 10^8 W/kg for dielectric capacitor), while their energy density is small (typically below 30 W·h/kg), which are usually used to generate a pulsed voltage or current. Figure 1 gives the diagram of power density as a function of energy density of above mentioned energy-stored devices.

Currently, the commercially used conventional dielectric capacitors are mainly made of dielectric polymers or dielectric ceramics, which usually have an energy density of $10^{-2} - 10^{-1}$ W·h/kg (less than 2 J/cm^3).[2,3] In contrast to conventional dielectric capacitors, although electrochemical supercapacitors have a moderate energy density, their power density still does not meet the requirement in some super-high-power electronics and systems, such as electric gun, directed energy weapon, active armor, and so on. Moreover, electrochemical supercapacitors usually also possess a complexed physical structure, a rather small maximum operating voltage (below 3.0 V), high leakage current of about microamperes (low energy efficiency) and limited cycling lift (10^5), which also prevent their application in some advanced pulsed power systems. Therefore, it could be concluded that, if the energy-storage density of the dielectric capacitors could be improved to be competitive with electrochemical supercapacitors or even batteries, their application field would be greatly expanded. For example, dielectric capacitors with high energy-storage density will further promote the compact electronic and electrical systems toward miniaturization, light weight, and integration.

Thus, propelled by the urgent demand of high power pulsed capacitors, the exploration on dielectric materials with improved electric energy-storage performance has attracted increasing attention, and quite a few work had been published. However, the overall summary on the research status of dielectric materials for high energy storage is still not carried out up to now. So, in present work, some physical principles are first applied to highlight the basic rules to explore the promising materials. Second, the energy-storage behaviors in four kind of most investigated dielectric materials,

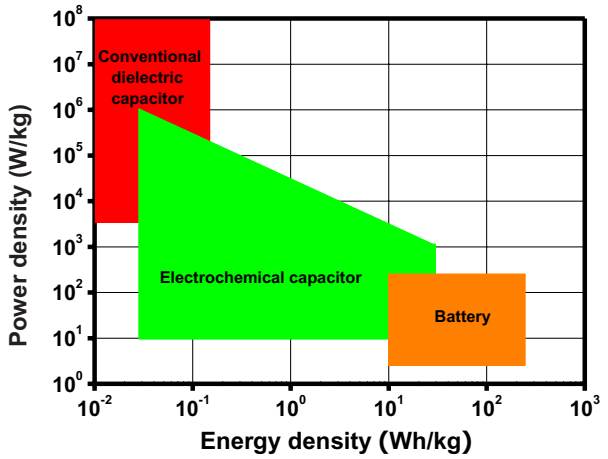

Fig. 1. Diagram of power density as a function of energy density in different energy-stored devices.

namely, antiferroelectrics, dielectric glass-ceramics, relaxor ferroelectrics and polymer-based ferroelectrics, are summarized, with a special attention on antiferroelectrics. Lastly, some general prospects are provided for future investigation. The aim of this review is to provide comprehensive information on research level of high energy-storage dielectric materials and to drive their potential application in practice.

2. Principles for High Energy-Storage in Dielectric Capacitors

2.1. *Basic knowledge on dielectric capacitor*

A capacitor typically consists of two conductor plates filled with certain dielectric materials, and is commonly in the parallel-plate form, as shown in Fig. 2. The electric energy storing is the function bases of capacitors in the electronics devices. The energy-stored ability of a capacitor is the so-called capacitance, which is only determined by the physical

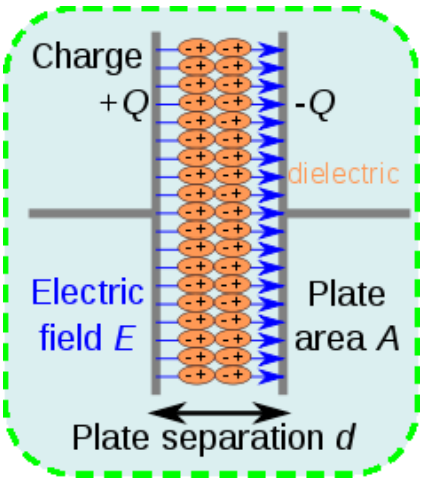

Fig. 2. The diagram of charge separation in parallel-plate capacitor under the function of electric field.

dimension (geometry) of the conductors and the permittivity of the dielectrics. It is independent of the potential difference between the conductors and the total charge on them. For example, the capacitance of a parallel-plate capacitor constructed of two parallel plates fulfilled with certain dielectrics is approximately equal to the following:

$$C = \varepsilon_r \varepsilon_0 \frac{A}{d}, \tag{1}$$

where C is the capacitance, A is the area of overlap of the two plates, ε_r is the relative permittivity, ε_0 is the electric constant ($\approx 8.85 \times 10^{-12} Fm^{-1}$), and d is the distance between the plates. Obviously, the capacitance is directly proportional to the overlap area of the conductor plates and the relative permittivity of the dielectrics, while inversely proportional to the separation distance between the plates.

As shown in Fig. 2, if an external voltage V is applied on the conductor plates, the electric polarization is happened. This will result in positives and negative charges with equal content accumulating on the two plates, respectively, which is the so-called charge process of the capacitor. The charge process will be finished when electrical potential caused by the accumulated charge $\pm Q$ on both plates is equal to the external applied voltage V. Q/V is equal to the capacitance C of the capacitor. Sometimes, the relative permittivity of the dielectrics is changed by the external bias, causing the capacitance to vary. In this case, capacitance is defined in terms of incremental change:

$$C = \frac{dq}{dv}. \tag{2}$$

During the charge process, the charges are moved between the conductor plates by the function of external bias, indicating that work must be done and that the electric energy is stored in the dielectrics at the same time. Hence, the amount of the stored energy W could be obtained from the following formula:

$$W = \int_0^Q V dq = \int_0^Q \frac{q}{C} dq = \frac{1}{2}\frac{Q^2}{C} = \frac{1}{2} CV^2 = \frac{1}{2} VQ. \tag{3}$$

2.2. *Measuring methods of energy-storage density for dielectric capacitor*

Commonly, for the convenience of comparison, the energy stored per unit volume of a dielectric J, namely energy-storage density, is often used in the research. Generally, J values could be obtained from two ways: static method and dynamic method.

Figure 3 gives the circuit for the measuring energy-storage density in static way.[4] In this case, the sample capacitor is first charged by an external bias, thus the electric energy is stored in the dielectric. Then, the capacitor is connected to the load R to complete a circuit by MOSFET switching. So part of the stored energy is discharged, accompanied by the

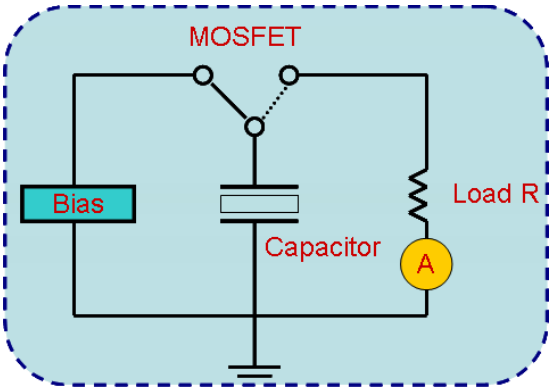

Fig. 3. The diagram of measurement circuit for the energy-storage density.

transient current formed in the closed circuit. According to the $I(t) - t$ curve, the discharged energy could be obtained by the following formula:

$$W = \int I^2(t)Rdt, \tag{4}$$

where R is the resistance of load, t is the discharged time. Finally, the energy density J could be calculated by using the ratio between W and the volume of capacitor. It should be noted here that the obtained J value in this way is the recoverable energy-storage density, because some stored energy is lost during the charge and discharge process.

As for the dynamic method, the energy-storage density could be induced from above formula (3). From the physics base, it could be known that the charge density (Q/A) on conductor plate of capacitor is equal to the electrical displacement D $(D = \varepsilon_0\varepsilon_r E)$ in the dielectrics. Thus, combining with formula (3), the energy-storage density J could be expressed as following:

$$J = \frac{W}{Ad} = \frac{\int_0^Q Vdq}{Ad} = \int_0^{E_{\max}} DdE, \tag{5}$$

where E is the external applied electrical field and equal to V/d, other letters are defined just as before. For the dielectrics with a high permittivity, the electrical displacement D is very close to their electrical polarization P. As a result, formula (5) can be rewritten as:

$$J = \int_0^{E_{\max}} PdE. \tag{6}$$

Evidently, based on formula (6), the J value of the dielectrics can be easily obtained by numerical integration of the area between the polarization and the curves of the electric field−polarization $(P - E)$ loops. As shown in Fig. 4(a), when the electric field increases from zero to the maximum $E_{\max}$, the polarization also increases to its maximum $P_{\max}$, and the electrical energy is stored in the capacitor as J_{store}, illustrated by the green and red area; during the discharge process from $E_{\max}$ to zero, the recoverable electrical energy

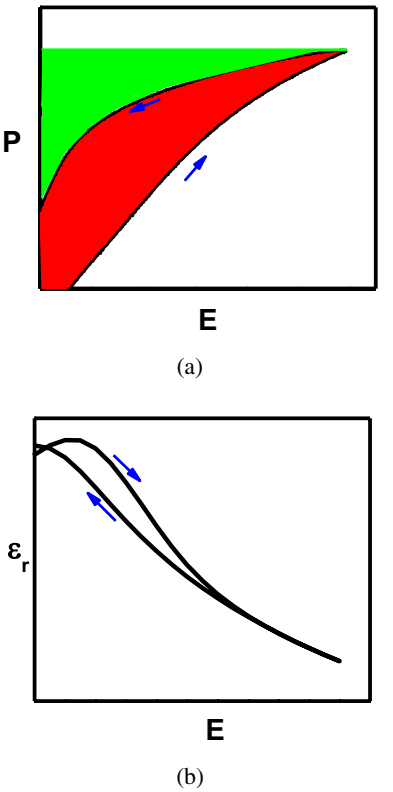

Fig. 4. (Color online) Typical dependence of (a) polarization and (b) permittivity on electric field of ferroelectrics in the first quarter.

density J_{reco} is then released, represented by the green area in the figure. This means that part of the stored energy (the red area enclosed by the loops) is exhausted during the depolarization process because of the hysteresis loss. Based on these results, the energy-storage efficiency η can be defined as:

$$\eta = \frac{J_{\text{reco}}}{J_{\text{store}}} \times 100\%. \tag{7}$$

Since the permittivity is defined as dP/dE, as shown in Fig. 4 (b), the formula (6) can be expressed as[5]:

$$J = \int_0^{E_{\max}} \varepsilon_0\varepsilon_r EdE. \tag{8}$$

For the linear dielectric materials, whose permittivity is independent of external applied field, the formula (5) could be simply expressed as following:

$$J = \int_0^{E_{\max}} PdE = \frac{1}{2}\varepsilon_0\varepsilon_r E^2. \tag{9}$$

This result indicates that the energy-storage density for the linear dielectric materials is directly proportional to the relative permittivity of the dielectrics and to the square of the operating field. It should be noted here that the J value obtained from dynamic way is usually larger than that from static way.

2.3. *Potential dielectrics for high energy-storage application*

According to above analysis, to design a proper dielectric material with high recoverable energy-storage density and high efficiency (small energy loss) for practical application, three requirements have to be satisfied simultaneously at least: high electric breakdown field, large saturated polarization, and small remnant polarization.[6] Figure 5 shows the typical $P-E$ loops and the energy-storage illustration of four kinds of dielectrics: (a) linear dielectric with constant permittivity (e.g., Al_2O_3, glass), (b) ferroelectric with spontaneous polarization (e.g., $BaTiO_3$, $PbTiO_3$), (c) relaxor ferroelectric with nanosized domains (e.g., $(Pb,La)(Zr,Ti)O_3$), and (d) antiferroelectric with zero net remnant polarization (e.g., $PbZrO_3$). Although, linear dielectrics usually possess higher breakdown field and lower energy loss, their smaller polarization value (permittivity) makes them not suitable for high energy-storage application. Ferroelectrics often have larger saturated polarization and moderate electric-field endurance, but their larger remnant polarization lead to a smaller energy-storage density and lower efficiency. Comparatively, as shown in Fig. 5, relaxor ferroelectrics and antiferroelectrics are more likely to be used for high energy storage because of their larger saturated polarization, smaller remnant polarization and moderate breakdown field. Meanwhile, with the development of new manufacturing processes of materials, such as glass-crystallization technique and composite technology, another two kinds of materials, glass-ceramic and polymer-based ferroelectrics, are also be found to have the potential for application in this area, which combine with the higher breakdown field of linear dielectric and larger polarization of ferroelectrics. Thus, in general, above mentioned four kinds of dielectrics: antiferroelectrics, dielectric glass-ceramics, relaxor ferroelectric and polymer-based ferroelectrics, are believed to be the most promising candidates for high energy-storage application, and quite a few works have been reported on these materials.

3. Energy-Storage Performance in the Well-Studied Materials

3.1. *Energy-storage in antiferroelectrics*

To understand the definition of antiferroelectrics, it is necessary to mention ferroelectrics because they have a close relationship in terms of polarization process. In ferroelectric materials, the adjacent dipoles in one domain share the same polarization orientation, and the orientation of dipoles can be changed to by the applied external dc electric field. Differently, in true antiferroelectric materials, the adjacent dipoles are aligned in opposite orientation, and under sufficient high dc electric-field the orientation of dipoles could be re-arrayed along direction of dc field and be changed into ferroelectric state, because of the smaller free energy between antiferroelectric and ferroelectric phase. Accordingly, antiferroelectrics could be defined as: spontaneous polarization direction of adjacent dipoles are opposite, and could be induced to same orientation under the function of electric-field.[7] Thus, as compared with ferroelectrics, antiferroelectrics

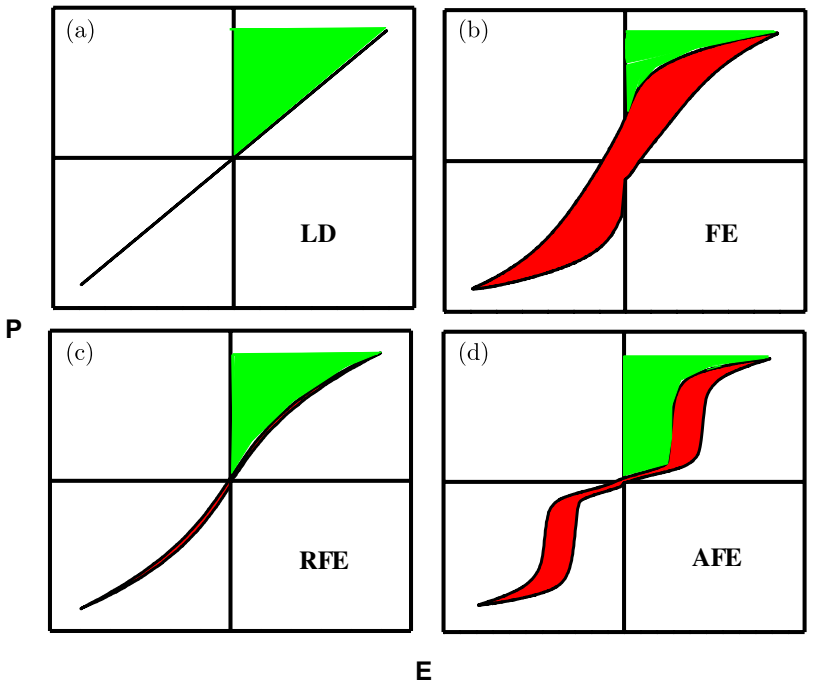

Fig. 5. (Color online) Diagram of hysteresis and energy storage density for (a) linear dielectrics, (b) ferroelectrics, (c) relaxor ferroelectrics, and (d) antiferroelectrics. The green area in the first quadrant is the recoverable energy density J_{reco}, and the red area is the energy loss J_{loss}.

possess two distinct features. One is that the net macroscopic remnant polarization is zero. Another is that $P-E$ curves under sufficient high electric field display double hysteresis loops.

In the group of antiferroelectric materials, generally there are several subcategories, such as perovskite group,[8] pyrochlore group,[8,9] liquid crystal,[10] and so on. Among all of these antiferroelectrics, materials with perovskite structure are the most important ones, which is usually expressed as ABO_3. Up to now, it have been proved that $PbZrO_3$, $PbHfO_3$, $NaNbO_3$ and their combinations are the typical antiferroelectrics with perovskite structure at room temperature.[11,12] Recently, $(Na_{0.5}Bi_{0.5})TiO_3-BaTiO_3$-based composites also showed antiferroelectric-like behavior in certain condition, such as, elevated temperature and/or special sintering atmosphere.

The history of study on energy storage in antiferroelectrics could be traced back to 1961, in which Jaffe predicated high energy-storage performance in $PbZrO_3$.[13,14] However, the energy-storage density in bulk antiferroelectric ceramics was usually less than 1 J/cm^3, owning to the lower breakdown field (below 60 kV/cm) caused by their interior defect in pores during the sintering route.[15,16] In 1971, a moderate recoverable energy density of 2.1 J/cm^3 was achieved in 65-μm-thick $PbZrO_3$ antiferroelectric thick films with a small amount of low-softening-point $SiO_2-Bi_2O_3$ glass by the screen-printing way.[5] Following this work, we investigated the energy-storage performance in 30 μm-thick $Pb_{0.97}La_{0.02}(Zr_{0.97}Ti_{0.03})O_3$ antiferroelectric films added with $PbO-B_2O_3-SiO_2-ZnO$ glass, which were also prepared by the screen-printing way.[17] As shown in Fig. 6, the addition of the glass is an efficient way to enhance the polarization and electric field endurance of the thick films. As a result, the largest recordable energy-storage density with a value of 3.1 J/cm^3 measured at 581 kV/cm was obtained in the 3-wt.%-glass added films at room temperature, which was 2.2 times higher than that of the pure films (1.4 J/cm^3). More interesting thing is that the energy-storage efficiency was also increased by the added glass. Although, as compared with bulk ceramic, the energy-storage performance was improved in the screen-printed thick films, the larger J_{reco} values was only about 3 J/cm^3, which was still caused by their pores-contained microstructure, as shown in the insert in Fig. 6. It could be concluded that, if a uniform and dense microstructure can be realized in the materials, a great improvement must be achieved.

Recently, with the rapid development of microelectronics devices toward miniaturization, lightweight and integration, thin film capacitors with improved performance are eagerly demanded. Moreover, dielectric materials in film form usually show an increased breakdown field, as compared with their bulk-ceramic counterpart. Thus, the studies on the energy-storage behaviors in antiferroelectric thin films are attracted increasing attention. A moderate energy storage density with a value of 7−8 J/cm^3 was reported in the thin

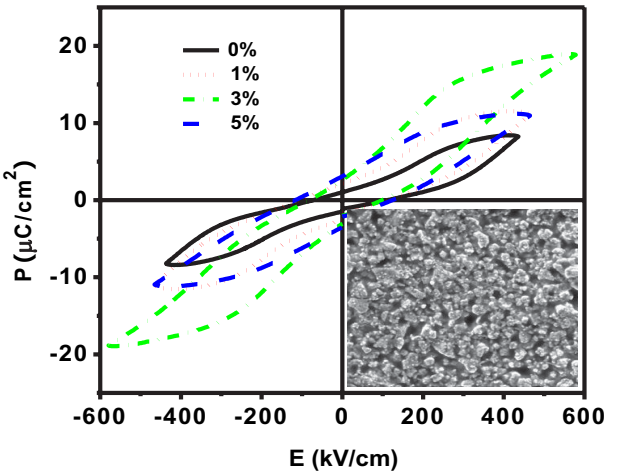

Fig. 6. The room-temperature $P-E$ loops of $Pb_{0.97}La_{0.02}(Zr_{0.97}Ti_{0.03})O_3$ anfiterroelectric thick films with different glass additions measured at their critical breakdown field. The insert shows SEM micrograph of the thick film with 3-wt.%-glass.

films on Pt-buffered silicon substrates by Xu *et al.* in 2000.[18] Following, Parui and Krupanidhi studied the energy storage performance in La-doped $PbZrO_3$ films with a thickness about 700 nm, a larger room temperature recoverable energy density of 14.9 J/cm^3 at 600 kV/cm was calculated in 5 mol.% La-doped films.[19] These results inspired the interest on the investigation on the energy-storage behavior in antiferroelectric films. Subsequently, we reported the improved energy storage performance of $PbZrO_3$ thin films (500 nm) by 5% Sr-doping.[20] Larger recoverable energy density J_{reco} of 14.5 J/cm^3 at 900 kV/cm at room temperature was obtained in Sr-doped $PbZrO_3$ films, corresponding to a higher energy efficiency η of 78%. An enhanced fatigue endurance and stable temperature-dependent energy storage performance were also observed in the Sr-doped $PbZrO_3$ thin films. Soon after, a maximum recoverable energy-storage density of 18.8 J/cm^3 at 900 kV/cm was achieved in 3 mol.% Eu-doped $PbZrO_3$ thin films.[21]

Beside, we also found that excess-lead content had a deep influence on the energy-storage density of antiferroelectric thin films.[22] It was found that J_{reco} value in 400-nm-thick $Pb_{0.97}La_{0.02}(Zr_{0.97}Ti_{0.03})TiO_3$ films at 1200 kV/cm was remarkably improved from 3.3 to 11.7 J/cm^3 by 20 mol.% excess lead adding. Mirshekarloo and co-authors studied the composition dependence of energy storage behaviors in $(Pb,La)(Zr,Sn,Ti)O_3$ antiferroelectric thin films with orthorhombic structure.[23] It was found that all the samples shared the similar J_{reco} value above 10 J/cm^3 at room temperature. More interestingly, very dense and uniform $(Pb_{0.92}La_{0.02})(Zr_{0.95}Ti_{0.05})O_3$ antiferroelectric thin films (about 1000 nm) were successfully fabricated on $LaNiO_3$-buffered Ni foil substrates via a chemical solution deposition way by Ma *et al.*[24,25] Excellent breakdown endurance (above 3500 kV/cm) can be realized in this film, and thus a considerable large J_{reco} value of 37 J/cm^3 was achieved.

Although, antiferroelectrics have a large energy-storage density, the overall stored energy is usually lower because of thickness limitation, which in some time could not meet the practical requirement. So, more recently, the energy-storage properties in the chemical-solution-derived antiferroelectric thick films with a thickness of 1−10 μm attract our interest, and some attempts have been tried.[26−28] We investigated the effects of heat treatment process on energy-storage performance of 3.3-μm $Pb_{0.97}La_{0.02}(Zr_{0.98}Ti_{0.02})O_3$ antiferroelectric thick films deposited on $LaNiO_3$/Si(100) substrates from polyvinylpyrrolidone (PVP)-modified chemical solution, in which each wet layer was first dried at 300°C, and then pyrolyzed at higher temperatures of 600°C, 650°C or 700°C, respectively. It was found that, on increasing the pyrolyzed temperature of single layer, the crystallized films displayed a more uniform and dense surface microstructure. As a result, the dielectric properties, antiferroelectric characterization and energy-storage performance were remarkably improved for the antiferroelectric films, as shown in Fig. 7. The maximum recoverable energy-storage density of 58.1 J/cm^3 and the energy-storage efficiency of 37.3% were obtained in the films pyrolyzed at 700°C for every layer. However, for the films fabricated from this way, as the thickness increase, their corresponding discharged energy-storage density and efficiency was declined because of their higher pores content. Based on these results, it is reasonably believed that good energy-storage properties could be achieved in the antiferroelectric thick films by further optimized process condition.

Apart from higher energy-storage density, antiferroelctrics also possess a higher charge releasing speed (the ferroelectric−antiferroelectric switching speed), which is an important parameter for their practical application. It was reported by Pan[29] that the ferroelectric−antiferroelectric switching time for $(Pb,La)(Zr,Sn,Ti)O_3$ bulk ceramics first gradually increased with the increase in applied electric field and then held the constant with an order of 1−2 μs, and that samples with larger switching field also had a larger switching speed. The electric field dependence of switching speed was supposed to be related with the stability of the induced ferroelectric phase. It was believed that the stability of the induced ferroelectric phase increased with increasing applied electric field and thus the energy barrier for the recovery of the antiferroelectric phase increased with increasing applied field. As a result, the switching time also increased. When the applied field is high enough to complete the antiferroelectric−ferroelectric transition, a further increase in the applied field would not increase the stability of the induced ferroelectric phase and thus the switching time levels off with increasing applied field. In recent studies, a higher charge releasing speed was observed in the lead-based ceramics by Zhang *et al.*[16] It is found that more than 80% stored electric charge can be released in 65 ns for the ceramic with a composition of $Pb_{0.925}La_{0.05}(Zr_{0.42}Sn_{0.40}Ti_{0.18})O_3$, and that this antiferroelectric ceramics capacitor can withstand 2000 times of charge−discharge cycling with no significant degradation of properties under 35 kV/cm, indicating a good fatigue endurance.

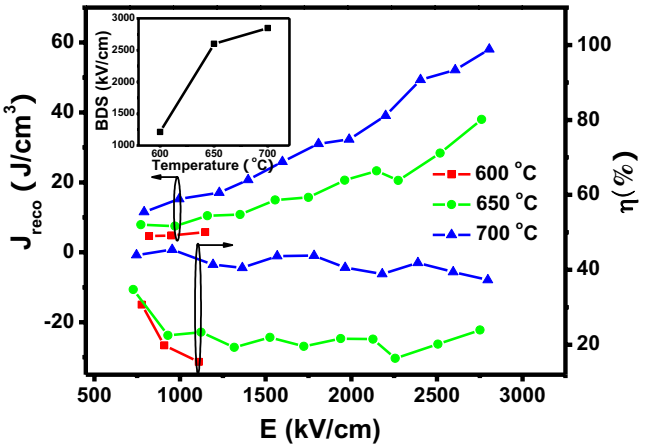

Fig. 7. Electric-field-dependent energy-storage density and energy-storage efficiency curves of the $Pb_{0.97}La_{0.02}(Zr_{0.98}Ti_{0.02})O_3$ thick films measured at room temperature and up to their critical breakdown field. The insert shows their room temperature breakdown field.

The ferroelectric−antiferroelectric switching speeds in antiferroelectric thin films were also investigated by several groups.[30−32] The typical work was reported by Bharadwaja and Krupanidhi[30] in which the electric field, temperature and thickness dependence of ferroelectric−antiferroelectric switching process were systemically studied in pure $PbZrO_3$ thin films. The results indicated that 60% of the stored energy in the 550-nm-thick films could be released in less than 7 ns at room temperature and at an applied electric field of 200 kV/cm. With further increase in the applied field, the switching time was slightly varied and the content of net released charge was increased. Whereas with increasing temperature, the switching time was reduced to 6 ns and the released charge was found to decrease. For the $PbZrO_3$ films with three different thicknesses of 250, 380 and 600 nm, at a fixed applied field of 200 kV/cm, the maximum released charge increased with the increase of the thickness, but the switching time had no obvious variation.

Derived by reducing the environment pollution of the toxic-lead element, the exploitation on energy storage in the lead-free antiferroelectric was attempted recently. The energy-storage properties of $0.89Bi_{0.5}Na_{0.5}TiO_3-0.06BaTiO_3-0.05K_{0.5}Na_{0.5}NbO_3$ lead free ceramics were carried out.[33−36] The dielectric measurement together with switching current curves indicated that a mixed ferroelectric and antiferroelectric phase transformed to a stable antiferroelectric when heating from 20°C to 90°C. In the stable antiferroelectric phase region, the J_{reco} under 56 kV/cm at 10 Hz maintained around 0.59 J/cm^3 from 100°C to 150°C. In addition, it was also found that the J_{reco} values were frequency independent from 1−63 Hz under 56 kV/cm. Although the obtained energy-storage density was quiet small and the stable antiferroelectric phase region existed only above 100°C, this work

is still meaningful because it highlighted the further way on studying the energy-storage in lead-free antiferroelectrics.

3.2. *Energy-storage in relaxor ferroelectrics*

Since their discovery by Smolensky and co-authors in 1954, the relaxor ferroelectrics or relaxors as a subclass of disordered crystals attracted continued interest because of their peculiar properties, such as large permittivity, high piezoelectric coefficient d_{33}, and large field-induced strain, which make them a candidate for application in advanced microelectronic devices.[37] In the past 60 years, quite a few relaxors have been confirmed, such as $Pb(Mg_{1/3}Nb_{2/3})O_3-PbTiO_3$, $(Pb,La)(Zr,Ti)O_3$, and $Ba(Ti,Sn)O_3$, and so on.[38,39] Generally speaking, the properties of relaxors are believed to be originated from their nanometer-size polar regions and their response to external stimuli. These polarization-related regions appear at "Burns" temperature T_D, which is usually far above the maximum point of permittivity T_m. A general feature of relaxors is the existence of quite wide peak in the temperature-dependent permittivity in which T_m is shifted to higher temperature as the measured frequency increases.

Moreover, under the function of external electric field, the polarization curves typically show a slim behavior with larger difference between saturation polarization and remnant polarization. The $P-E$ loops of relaxors also show a decay of polarization with temperature because of their diffused phase switching. These characteristics make relaxors possess the possibility for application in high energy storage.[40] However, the studies on energy storage in relaxor are rarely carried out due to the low breakdown field of bulk ceramics. Recently, the energy-storage behavior in relaxor thin films has received some interest, derived by the demand in thin film capacitors. In 2011, Yao and co-authors successfully prepared the $0.462Pb(Zn_{1/3}Nb_{2/3})O_3-0.308Pb(Mg_{1/3}Nb_{2/3})O_3-0.23PbTiO_3$ relaxor thin films by PEG-assisted chemical solution way.[1] It was observed that the films showed a larger maximum polarization of 108 $\mu C/cm^2$ and a moderate remnant polarization of 20 $\mu C/cm^2$ at an electric field of 700 kV/cm. As a result, a larger recoverable energy-storage density of 15.8 J/cm^3 was obtained in this film. Following, Kwon and Lee studied the energy-storage performance in 500-nm-thick $(1-x)BaTiO_3-xBi(Mg,Ti)O_3 (0.1 \leq x \leq 0.15)$ films.[41] The crystallized relaxor films showed nearly linear polarization response and possess an average breakdown field as high as 2.17 MV/cm. The larger J_{reco} of 37 J/cm^3 was obtained in $0.88BaTiO_3-0.12Bi(Mg,Ti)O_3$ composite films with a good stability from room temperature to 200°C. Differently, Ortega and co-authors reported the energy storage in 600-nm-thick $BaTiO_3/Ba_{0.3}Sr_{0.7}TiO_3$ relaxors superlattices grown on (100) MgO single crystal substrates by pulsed laser deposition.[42] The current–field results illustrated that the thin films had a very high breakdown field of 5.8–6 MV/cm with a low leakage current density of 10–35 mA/cm^2, indicating that a higher recoverable energy-storage density of 46 J/cm^3 could be achieved in this film.

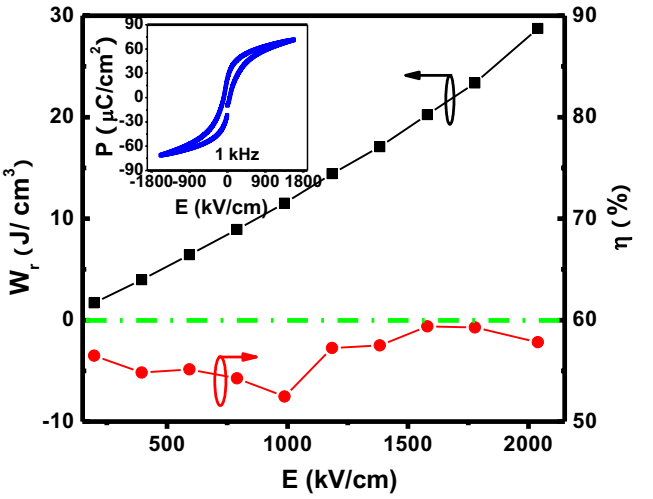

Fig. 8. The electric field dependence of energy-storage density and energy-storage efficiency of $(Pb_{0.91}La_{0.09})(Zr_{0.65}Ti_{0.35})O_3$ thin film measured at room temperature and 1 kHz. The insert shows $P-E$ loop of the thin film measured at room temperature and at 1 kHz.

Inspired by these interesting results, we investigated the dielectric properties and energy-storage performance in the typical $(Pb_{0.91}La_{0.09})(Zr_{0.65}Ti_{0.35})O_3$ relaxor ferroelectric in thin-film form, which were grown on platinum-buffered silicon substrates via a sol–gel technique.[43] The crystallized films with a thickness of about 1000 nm showed a random orientation with uniform and dense macrostructure. A considerable capacitance density of 925 nF/cm^2 at 1 MHz and a higher critical breakdown field of 2177 kV/cm were realized in thin film. As shown in Fig. 8, this relaxor film also possessed a slim $P-E$ loop with a larger difference between the saturated polarization and the remnant polarization, which was 49.1 $\mu C/cm^2$ at 1580 kV/cm. As the external field increased from 200 to 2040 kV/cm, the recoverable energy-storage density at 1 kHz was raised from 1.7 to 28.7 J/cm^3. However, the energy efficiency showed a good stability and varied between 52.4% and 59.4% in the measurement range. We also found that the relaxor thin films possessed a good temperature and frequency-dependent stability. All of these results further demonstrate that relaxor ferroelectrics is a promising candidate for high energy-storage application.

3.3. *Energy-storage in glass-ceramic*

Broadly, glass-ceramic can be defined as a composite of an amorphous phase and one or more crystalline phase, as shown in Fig. 9. This kind of materials usually shares the properties with both glasses and ceramics. Commonly, glass-ceramic can be synthesized in two different ways: composite method and body crystallization method.[44,45] In the former, the desired glass and ceramic powders are first prepared, respectively; then they are mixed with determined ratio and pressed into certain shapes; finally, the compositions are sintered at certain temperature to form the product.

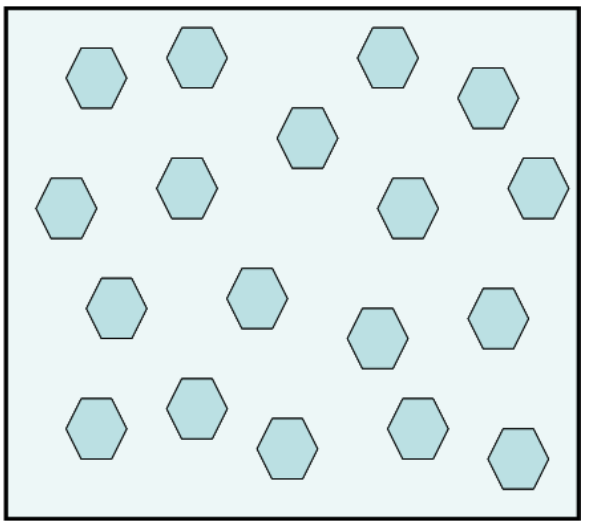

Fig. 9. The diagram of glass-ceramic system. The hexagon region and the white area are taken as ceramic phase and glass phase, respectively.

Glass-ceramics synthesized in this way usually possess ideal compositions, but some pores are often formed. In the latter, an amorphous phase with desired chemical elements is first fabricated by the typical glass-manufacturing process; then, after cooling and shaping, the amorphous are partly crystallized at certain temperature to obtain the final glass-ceramic. In this case, a pore-free microstructure can be easily obtained in the glass-ceramics, but their composition is hard to be selected.

Therefore, by properly controlling the chemical composition of amorphous phase and crystalline phase, high electric breakdown field and larger permittivity can be realized simultaneously in a glass-ceramic system, indicating that a high energy-storage density could be achieved in these materials. However, it should be noted here that the much interface is usually existed between the amorphous phase and crystalline phase, which will produce an adverse influence on the energy discharge.

The investigation on the energy storage of glass-ceramics prepared from composite method were mainly focused on $BaTiO_3$-based ceramics, such as (Ba,Sr)TiO_3 and (Ba,Zr)TiO_3−(Ba,Ca)TiO_3.[44,46–48] The typical example was given by Zhang and co-authors in which $Ba_{0.4}Sr_{0.6}TiO_3$ ceramics with the addition of 5−20 vol.% $BaO-SiO_2-B_2O_3$ glass were prepared.[44] It was observed that, on increasing the glass content, the grain size, permittivity, and polarization values of the glass-ceramics declined gradually and linear $P-E$ loops were obtained, but their electric breakdown field was enhanced due to the reduction of the porosity and pore size. The largest breakdown field of 240 kV/cm was realized in 20 vol.%-glass added ceramics. As a overall result, the samples with 5 vol.%-glass addition had the highest recoverable energy-storage density of 0.89 J/cm^3, which is 2.4 times higher than that of pure $Ba_{0.4}Sr_{0.6}TiO_3$ ceramics (0.37 J/cm^3). Following, Chen and co-authors studied the effects of $SrO-B_2O_3-SiO_2$ glass additive on the energy-storage properties of $Ba_{0.4}Sr_{0.6}TiO_3$ ceramics.[47] Similar results were obtained in this work. The dielectric breakdown strength (about 150 kV/cm) of the glass-ceramics was improved to about twice by 10 wt.% glass addition, in contrast to pure ceramics. The maximum discharged energy-storage density of 0.44 J/cm^3 was achieved in 2 wt.% glass added ceramics. From above reports, it can be found that, although the glass additive can improve the breakdown strength, they also lead to a declination of the maximum polarization. Thus, in order to obtain the largest energy-storage density, the glass content should be properly controlled.

Comparatively, the body crystallization method is a more widely used way to synthesize glass-ceramics for high energy storage. Currently, (Ba,Sr)TiO_3 and $NaNbO_3$-based glass-ceramics are the widely studied systems.[49–52] Gorzkowski and co-authors explored the energy storage properties of $BaO-SrO-TiO_2-Al_2O_3-SiO_2$ glass-ceramics with (Ba,Sr)TiO_3 phase.[49] A relative permittivity of 1000 and a breakdown field of 800 kV/cm were achieved; however, the recoverable energy-storage density from $P-E$ results was only 0.3−0.9 J/cm^3, because of the large hysteresis loss. Following, the systematic works on $BaO-SrO-TiO_2-Al_2O_3-SiO_2$ system were carried out by Zhang's group.[50] It was found that sintering temperature had a deep influence on the phase composition and their dielectric properties. The (Ba,Sr)TiO_3 phase was from after annealed at 830°C, and the degree of crystallinity was increased with increasing annealing temperature from 830−950°C. The maximum J_{reco} of 0.18 J/cm^3 was obtained at 280 kV/cm. Moreover, they also reported that MnO_2 and AlF_3 were the efficient additives to optimize the microstructure and energy-storage properties of this kind of glass-ceramics.[53,54] In their work, all the obtained recoverable energy-storage density was below 0.2 J/cm^3, although good electric breakdown strength and moderate permittivity were achieved in the glass-ceramics. The authors indicated that it was caused by the interfacial polarization between amorphous phase and crystalline phase, which had a long relaxation process.[50] As showed in Fig. 10, with the increase of interfacial polarization, more charges can be stored and thus resulting in an increase of overall energy density in the charging process. However, these excess charges are trapped due to the long relaxation process of interfacial polarization in the discharge circle. Consequently, lower discharged energy density and lower energy efficiency are attainable notwithstanding a higher overall charge energy density. These results were further demonstrated by Du's group in $NaNbO_3$-based glass-ceramics.[51,55,56] A huge energy as high as 17 J/cm^3 was stored in $Na_2O-PbO-Nb_2O_5-SiO_2$ glass-ceramic ($NaNbO_3$ and $Pb2Nb_2O_7$ phase), but only few could be released in fact.[51] They also pointed out that composition control as well as electrode structure design were useful methods to tailor the energy-storage properties of glass-ceramics. For example, by adding La_2O_3

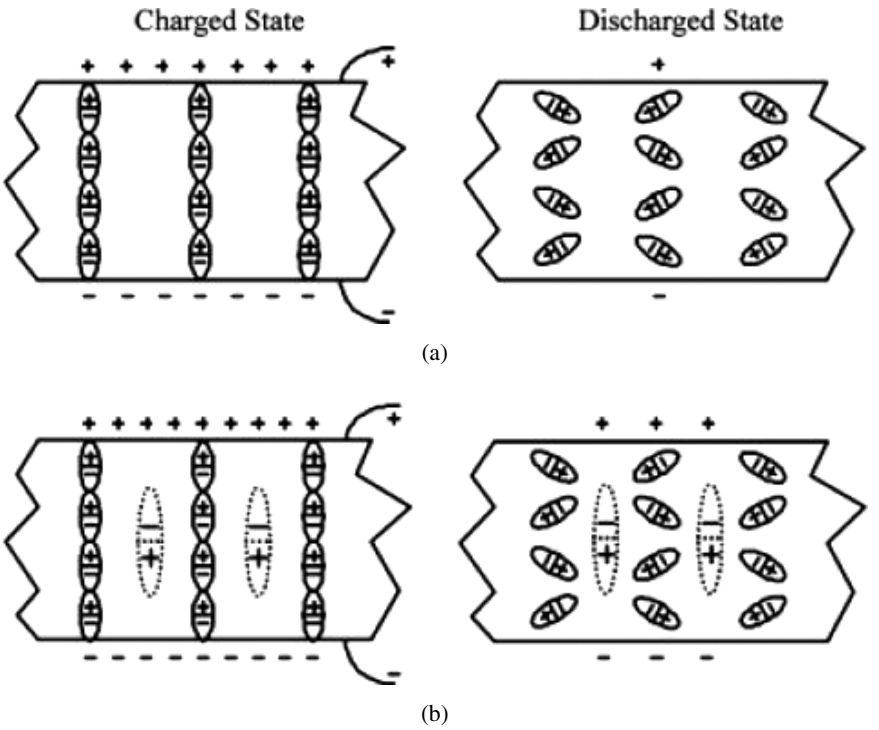

Fig. 10. The Schematic of the charge and discharge mechanism in a dielectric capacitor: (a) without interfacial polarization and (b) with interfacial polarization. (Reprinted with kind permission from Ref. 50.)

into $Na_2O-BaO-Nb_2O_5-SiO_2$ system, the permittivity, breakdown field, and polarization value of the glass-ceramic ($NaNbO_3$, $Ba_2NaNb_5O_{15}$ phase) were all increased greatly.[55] The largest recoverable energy-storage density of 1.2 J/cm^3 was achieved in 2 mol.% La_2O_3 added glass-ceramic at 280 kV/cm. More recently, they observed that, in $ANb_2O_6-NaNbO_3-SiO_2$ ($A = [(1-x)Pb, xSr]$) glass-ceramic, the highest J_{reco} of 2.27 J/cm^3 was realized at the point of $x = 0.6$, which was twice higher than those of the end-products (i.e., $x = 0$ and $x = 1$).[56]

3.4. *Energy-storage in polymer-based ferroelectrics*

Last but not least, the energy-storage performance in polymer-based materials will be presented in this section. Actually, compared with above three kinds of dielectrics, much more attention has been paid on polymer by the worldwide researchers, because of their super-high breakdown field, lower fabricating temperature, and the good flexibility. Up to now, quite a few papers have been published on the energy storage in polymer, including polypropylene (PP), polyester (PT), polycarbonate (PC), polyimide, aromatic polyurea, aromatic polythiourea (ArPTU), polyvinylidene-fluoride (PVDF), and their related composites, and so on.[57–60] Among these polymers, PVDF-based materials are the most studied ones due to the larger permittivity caused by their ferroelectric nature, and several reviews have been reported.[61–65] Thus, here, for the completeness of this work and at the same time for avoiding the repeat, we only give a brief summary on the energy-storage behavior in PVDF-based materials, including: pure PVDF, PVDF-based copolymers, and polymer/inorganic composites.

In general, four different crystalline phases in PVDF are detected, including α [in trans-gauche conformation (TGTG)], β [in all trans planar zigzag conformation (TTTT)], γ [in a conformation of three trans linked to a gauche (TTTG), and δ phase (a polar version of the α phase), as shown in Fig. 11.[58,64] Among them, the α phase is nonpolar and the β, γ, and δ phase are ferroelectric. Comparatively, the β phase possesses the largest spontaneous polarization due to its large dipole moment. The α phase is obtained by cooling the melt and drying below at a normal rate, the δ phase is formed by poling the α phase sample under an electric field of 100–200 MV/m. The γ phase is often achieved by drying polar solvent below 100°C or annealing/crystallization at high temperatures. The β phase can be realized by mechanical stretching or high field poling (4–5 MV/cm) of α or γ form samples. It is well known that the energy-storage properties of dielectrics have a close relation with their phase structure. Li and co-authors studied energy-storage of PVDF in α, β, and γ forms.[58] It was found that, although the samples in three phases possessed the similar energy-storage density of 1.5 J/cm^3 and loss under low electric field, γ phase samples have the largest discharged energy-storage density of 14 J/cm^3 because of their highest breakdown field of 5 MV/cm.

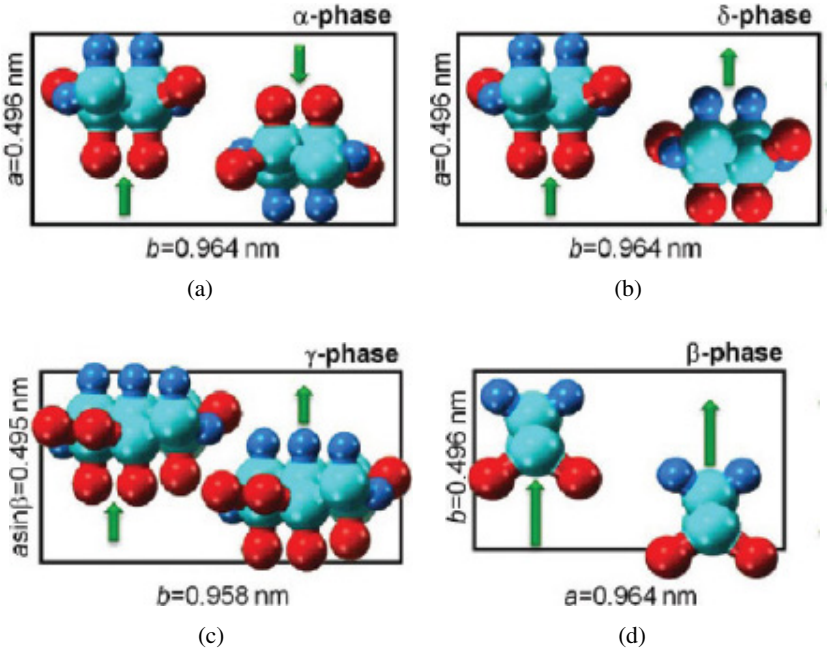

Fig. 11. Unit cell of (a) α, (b) δ, (c) γ , and (d) β phase of PVDF crystal viewed along the c-axes. (Reprinted with kind permission from Ref. 64.)

In order to increase the difference between the saturated polarization and remnant polarization and the breakdown field for optimizing the energy-storage properties of PVDF, some other organic groups are introduced to form PVDF-based copolymer and terpolymer. Currently, the involved bulk group are mainly chlorotrifluoroethylene (CTEE), hexafluoropeoptlene (HFP), trifluoroethylene (TrFE), vinylidene fluoride (VDF), and so on.[66−80] It was first proved in 2006 by Chu and co-authors that a high recoverable energy-storage density of 17 J/cm^3 was realized in P(VDF-CTEE) 91/9 mol.% at 5.75 MV/cm.[66] Following, by further improving the processing condition and copolymer film quality, a huge release energy-storage density of about 25 J/cm^3 was obtained in this copolymer with a thickness of 10 μm at 700 kV/cm.[76] Another typical example was given by Rahimabady and co-authors.[72] They obtained a discharged energy-storage density of 27 J/cm^3 at 8.68 MV/cm in VDF oligomer/PVDF (80/20) films, which is the highest reported value up to now. From the reported results, it is concluded that the energy-storage properties can be tailored by their chemical composition, growth orientation, stress, crystalline properties, and so on.

Although these polymers possess good electric field endurance, the lower relative permittivity (usually below 20) limits the further improvement of their energy-storage density. Differently, some oxides (such as ferroelectrics) show ultra-high dielectric permittivity. So, a composite integrating a high permittivity from a ceramic with a high breakdown field from a polymer might be realized by introducing ceramics (particle and fiber form) into the polymer. As a result, lots of attempts were tried, the involved ceramics including TiO_2, MnO_2, ZrO_2, $BaTiO_3$, $(Ba,Sr)TiO_3$, $Pb(Zr,Ti)O_3$, $CaCu_3Ti_4O_{12}$, and so on.[81−88] It was found that the composites have an increased permittivity in contrast to their polymer host matrix, but in some cases they also displayed decreased breakdown strength and raised energy loss. A general reason is the agglomeration and phase separation from the matrix due to the high surface energy of dielectric ceramics, resulting in a high defect density in the composite. Therefore, in order to improve their distribution in the polymer matrix, the surface of fillers commonly need to be modified by using a chemical method. A typical work on the energy-storage properties of inorganic fillers/polymer systems were given by Yu and co-authors.[89] In this work, homogeneous $BaTiO_3$−PVDF nanocomopsites films were successfully fabricated, in which $BaTiO_3$ particles were first treated by the agent NXT-105. On increasing $BaTiO_3$ particles from 0 to 50 vol.%, the relative permittivity of the composite was gradually increased from 9.9 to 53.9. Accordingly, both the dielectric displacement and the energy-storage density were enlarged, in contrast to their PVDF matrix, as shown in Fig. 12. Under the electric field of 2 MV/cm, the discharge energy-storage density of the nanocomposite with 20 vol.% $BaTiO_3$ addition was 3.54 J/cm^3, which was 46% higher than that of the pure PVDF polymer (2.42 J/cm^3). Moreover, the higher $BaTiO_3$ content also lead to a sharp reduction of the breakdown field, caused by the increasing defect in the samples. So, it is expected that the composite under the optimum energy-storage condition could possess the ceramic fillers as small as possible. An efficient way to realize this aim is to control the shape of the fillers, proposed by Song and co-authors very recently.[90−92]

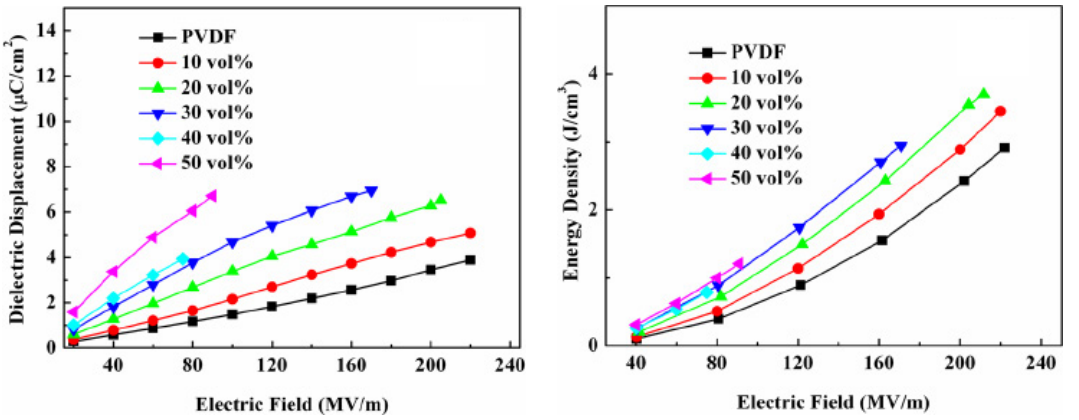

(a) (b)

Fig. 12. The dielectric displacement (a) and energy density (b) of the pure PVDF and the nanacomposites as a function of the volume fraction of $BaTiO_3$. (Reprinted with kind permission from Ref. 89.)

As reported in their studies, in contrast to spherical particles, the fibers possessed two advantages: (1) they were capable of increasing the dielectric permittivity of the composites at much lower volume fraction due to their large dipole moments, and (2) their morphology also were good to reduce the surface energy, which prevented the fillers agglomerating in the polymer matrix. For example, only by introducing 4.4 vol.% dopamine-modified $Ba_{0.6}Sr_{0.4}TiO_3$ nanofibers into PVDF, a maximum discharged energy-storage density of 5.24 J/cm^3 was achieved, which is more than doubled that of the pure PVDF (2.45 J/cm^3). These results indicated that, by proper morphology control of the ceramic, the good energy-storage properties could be further improved under optimizing conditions.

4. Future Prospects

According to above summarized results, we can conclude that some interesting achievements have been obtained in high energy-storage materials, but there still exist many problems need to be solved in order to propel the application of energy-storage capacitors in practice. So, in this part, we will present some key aspects to throw further light on the investigation in this area.

As reported, because of their lower breakdown strength, the final recoverable energy-storage density in antiferroelectric and relaxor ferroelectric bulk ceramics is still very smaller and is below 1 J/cm^3, which cannot meet the practical requirements. Although the huge discharged energy-storage density of 50 J/cm^3 in antiferroelectric and 30 J/cm^3 in relaxors have been achieved in their thin film form ($< 1\ \mu$m), the overall stored energy is every small due to their thin-thickness limitation and do not meet the requirement in some cases. So, the development of bulk ceramics or thick films ($1-100\ \mu$m) with a breakdown field comparative to their thin film form may be an urgent way to increase their energy-storage density and overall stored energy. Another more promising way is to exploit their multilayer ceramic capacitors (MLCC), caused by the huge achievement in MLCC with a layer thickness as thin as 1 μm. As for glass-ceramic and polymer-based dielectrics, the much interface existed in their body is a main obstacle to improve energy-storage density and efficiency. So, the deep study on the polarization mechanism at interface is necessary to take proper way for increasing breakdown field and decreasing interface loss. Moreover, the fabrication process should be further optimized to control the permittivity and to modify the interface in glass-ceramic and inorganic-polymer systems. Besides, the environment-friendly new dielectric materials with good energy-storage properties should be explored. It is especially important to antiferroelectrics and relaxor ferroelectrics because they are usually lead based.

Currently, the investigation is mainly focused on the improvement of energy-storage density in these dielectrics, but their energy efficiency, charge and discharge speed, fatigue behavior, temperature stability and lifetime are often neglected. In fact, these parameters are also very important for their application in capacitors. So, these aspects have to be addressed in the future study. Moreover, the energy-storage density is usually obtained from dynamic method, i.e., from the P−E loops, which is higher than that from static way. However, up to now, to the best of our knowledge, there is no such commercial equipment to be supplied because of requirement of super-accurate resolution of the time. Therefore, the design of the special equipment in static way may be also a meaningful work for high energy-storage investigation.

5. Summary

In summary, we briefly reviewed the current state of the study on high energy-storage dielectrics. Significant progress has been made in the four kinds of dielectric materials, mainly including antiferroelectrics, relaxor ferroelectrics,

glass-ceramics, and polymer-based ferroelectrics. Currently, improving or modifying the difference between the saturated polarization and the remnant polarization and higher electric breakdown field are the key tasks to optimize the energy-storage performance in these dielectric materials. Because of their excellent electric field strength, huge energy-storage density was achieved in antiferroelectric and relaxor thin films. Although glass-ceramics possess higher breakdown field and moderate permittivity, a small discharge energy-storage density below 3 J/cm^3 was produced, caused by the larger polarization loss at the interface between glass phase and ceramic phase. Comparatively, energy-storage properties in polymer-based materials received more attention. Several techniques, such as, growth orientation, stress phase control, composite, and so on, have been employed to optimize their energy-storage performance. The highest discharged energy-storage density 27 J/cm^3 is obtained in VDF oligomer/PVDF films. Finally, based on the current research state in these materials, some possible ways were proposed to further improve the energy-storage behaviors. Moreover, some rarely studied parameters on the energy storage were also addressed to meet practice requirements. Overall, we hope that this review has captured the exciting new development in this area and also can throw further light on the matter.

Acknowledgments

The authors would like to acknowledge the financial support from the National Natural Science Foundation of China under grant No. 51002071, the Program for New Century Excellent Talents in University, and the Program for Young Talents of Science and Technology in Universities of Inner Mongolia Autonomous Region.

References

[1]K. Yao, S. Chen, M. Rahimabady, M. S. Mirshekarloo, S. Yu, F. E. H. Tay, T. Sritharan and L. Lu, Nonlinear dielectric thin films for high-power electric storage with energy density comparable with electrochemical supercapacitores, *IEEE Trans. Ultrason., Ferroelectr., and Freq. Control* **58**, 19568 (2011).

[2]W. J. Sarjenat, J. Zirnheld and F. W. Macdougall, *IEEE Trans. Plasma Sci.* **26**, 1368 (1998).

[3]G. R. Love, Energy storage in ceramic dielectrics, *J. American Ceram. Soc.* **73**, 323 (1990).

[4]X. Chen, H. Zhang, F. Cao, G. Wang, X. Dong, Y. Gu, H. He and Y. Liu, Charge-discharge properties of lead zirconate stannate titanate ceramics, *J. Appl. Phys.* **106**, 034105-1 (2009).

[5]I. Burn and D. M. Smyth, Energy storage in ceramic dielectrics, *J. Mater. Sci.* **7**, 339 (1972).

[6]N. H. Fletcher, A. D. Hilton and B. W. Ricketts, Optimization of energy storage density in ceramic capacitors, *J. Phys. D: Appl. Phys.* **29**, 253 (1996).

[7]J. Zhai, X. Li and H. Chen, Effect of orientation on the ferroelectric-antiferroelectric behavior of sol-gel deposited (Pb,Nb)(Zr, Sn,Ti)O_3 thin films, *Thin Solid Films* **446**, 200 (2004).

[8]E. C. Subbarao, Ferroelectric and antiferroelectric materials, *Ferroelectrics* **5**, 267 (1973).

[9]D. Bernard, J. Pannetier and J. Lucas, Ferroelectric and antiferroelectric materials with pyrochlore structure, *Ferroelectrics* **21**, 429 (1978).

[10]I. Nishiyama, Antiferroelectric liquid crystals, *Adv. Mater.* **6**, 966 (1994).

[11]G. A. Samara, Pressure and temperature dependence of the dielectric properties and phase transition of the antiferroelectric perovskites: $PbZrO_3$ and $PbHfO_3$, *Phys. Rev. B* **1**, 3777 (1970).

[12]O. A. Zhelnova and O. E. Fesenko, Phase transitions and twinning in $NaNbO_3$ crystals, *Ferroelectrics* **75**, 465 (1987).

[13]B. Jaffe, Antiferroelectric ceramics with field-enforced transition: A new nonlinear circuit element, *Proc. IRE* **49**, 1264 (1961).

[14]K. Singh, Antiferroelectric lead zirconate, a material for energy storage, *Ferroelectrics* **94**, 433 (1989).

[15]X. Chen, F. Cao, H. Zhang, G. Yu, G. Wang, X. Dong, Y. Gu, H. He and Y. Liu, Dynamic hysteresis and scaling behavior of energy density in $Pb_{0.99}Nb_{0.02}[(Zr_{0.60}Sn_{0.40})_{0.95}Ti_{0.05}]O_3$ antiferroelectric bulk ceramics, *J. Am. Ceram. Soc.* **95**, 1163 (2012).

[16]H. Zhang, X. Chen, F. Cao, G. Wang and X. Dong, Charge-discharge properties of antiferroelectric ceramics capacitor under different electric fields, *J. Am. Ceram. Soc.* **93**, 4015 (2010).

[17]X. Hao, P. Wang, X. Zhang and J. Xu, Microstructure and improved energy-storage performance of PbO-B_2O_3-SiO_2-ZnO glass added $(Pb_{0.97}La_{0.02})(Zr_{0.97}Ti_{0.03})O_3$ antiferroelectric thick films, *Mater. Res. Bull.* **48**, 84 (2013).

[18]B. Xu, Y. Ye, Q.-M. Wang, N. G. Pa and L. E. Cross, Effect of compositional variations electrical properties in phase switching (Pb,La)(Zr,Ti,Sn)O_3 thin and thick films, *J. Mater. Sci.* **35**, 6027 (2000).

[19]J. Parui and S. B. Krupanidhi, Enhancement of charge and energy storage in sol-gel pure and La-modified $PbZrO_3$ thin films, *Appl. Phys. Lett.* **92**, 192901-1 (2008).

[20]X. Hao, J. Zhai and X. Yao, Improved energy storage performance and fatigue endurance of Sr-doped $PbZrO_3$ antiferroelectric thin films, *J. Am. Ceram. Soc.* **92**, 1133 (2009).

[21]M. Ye, Q. Sun, X. Chen, Z. Jiang and F. Wang, Effect of Eu doping on the electrical properties and energy storage performance of $PbZrO_3$ antiferroelectric thin films, *J. Am. Ceram. Soc.* **95**, 1486 (2012).

[22]X. Hao, J. Zhou and S. An, Effects of PbO content on the dielectric properties and energy storage performance of $(Pb_{0.97}La_{0.02})(Zr_{0.97}Ti_{0.03})O_3$ antiferroelectric thin films, *J. Am. Ceram. Soc.* **94**, 1647 (2011).

[23]M. S. Mirsheklarloo, K. Yao and T. Sirtharan, Large strain and high energy storage density in orthorhombic perovskite $(Pb_{0.97}La_{0.02})(Zr_{1-x-y}Sn_xTi_y)O_3$ antiferroelectric thin films, *Appl. Phys. Lett.* **97**, 14902-1 (2010).

[24]B. Ma, D.-K. Kwon, M. Narayanan and U. Balachandran, Fabrication of antiferroelectric PLZT films on metal foils, *Mater. Res. Bull.* **44**, 11 (2009).

[25]B. Ma, D.-K. Kwon, M. Narayanan and U. Balachandran, Dielectric properties and energy storage capability of antiferroelectric $Pb_{0.92}La_{0.08}Zr_{0.95}Ti_{0.05}O_3$ film-on-foil capacitors, *J. Mater. Res.* **24**, 2993 (2009).

[26]X. Hao, Z. Yue, J. Xu, S. An and C. Nan, Energy storage performance and electrocaloric effect in (100)-preferred $Pb_{0.97}La_{0.02}(Zr_{0.95}Ti_{0.05})O_3$ antiferroelectric thick films, *J. Appl. Phys.* **110**, 064109-1 (2011).

[27]Y. Wang, X. Hao and J. Xu, Effects of PbO-insert layer on the microstructure and energy storage performance of (042)-preferred PLZT antiferroelectric thick films, *J. Mater. Res.* **27**, 1770 (2012).
[28]Y. Wang, X. Hao, J. Yang, J. Xu and D. Zhao, Fabrication and energy-storage performance of PLZT antiferroelectric thick films derived from PVP-modified chemical solution, *J. Appl. Phys.* **112**, 034105-1 (2012).
[29]W. Y. Pan, C. Q. Dam, Q. M. Zhang and L. E. Cross, "Large displacement transducers based on electric field forced phase transitions in the tetragonal $(Pb_{0.97}La_{0.02}(Ti,Zr,Sn)O_3$ family of ceramics", *J. Appl. Phys.* **66**, 6014 (1988).
[30]S. S. N. Bharadwaja and S. B. Krupanidhi, Backward switching phenomenon form field forced ferroelectric to antiferroelectric phases in antiferroelectric $PbZrO_3$ thin films, *J. Appl. Phys.* **89**, 4541 (2001).
[31]B. Xu, P. Moses, N. G. Pai and L. E. Cross, Charge release of lanthanum-doped zirconate titanate stannate antiferroelectric thin films, *Appl. Phys. Lett.* **72**, 593 (1998).
[32]K. G. Brooks, J. Chen, K. R. Udayakumar and L. E. Cross, Electric field forced phase switching in La-modified lead zirconate titanate stannate thin films, *J. Appl. Phys.* **75**, 1699 (1994).
[33]J. Fu and R. Zuo, Polizriation reversal and dynamic scaling of $(Na_{0.5}K_{0.5})NbO_3$ lead free ferroelectric ceramics with double hysteresis-like loops, *J. Appl. Phys.* **112**, 104114-1 (2012).
[34]G. Viola, H. Ning, M. J. Reece, R. Wilson, T. M. Correia, P. Weaver, M. G. Cain and H. Yan, Reversibility in electric field-induced transitions and energy storage properties of bismuth-based perovskite ceramics, *J. Phys. D: Appl. Phys.* **45**, 355302-1 (2012).
[35]F. Gao, X. Dong, C. Mao, F. Cao and G. Wang, c/a ratio-dependent energy-storage density in $(0.9\text{-}x)Bi_{0.5}Na_{0.5}TiO_3$-$xBaTiO_3$-$0.1K_{0.5}Na_{0.5}NbO_3$ ceramics, *J. Am. Ceram. Soc.* **94**, 4162 (2011).
[36]F. Gao, X. Dong, C. Mao, W. Liu, H. Zhang, L. Yang, F. Cao and G. Wang, Energy-storage properties of $0.89Bi_{0.5}Na_{0.5}TiO_3$-$0.06BaTiO_3$-$0.05K_{0.5}Na_{0.5}NbO_3$ lead-free anti-ferroelectric caermaics, *J. Am. Ceram. Soc.* **94**, 4382 (2011).
[37]V. V. Shvartsman and D. C. Lupascu, Lead-free relaxor ferroelectrics, *J. Am. Ceram. Soc.* **95**, 1 (2012).
[38]L. E. Cross, Relaxor ferroelectrics: An overview, *Ferroelectrics* **151**, 305 (1994).
[39]A. A. Bokov and Z.-G. Ye, Recent progress in relaxor ferroelectrics with perovskite structure, *J. Mater. Sci.* **41**, 31 (2006).
[40]M. Narayanan, U. Balachandran, S. Stoupin, B. Ma, S. Tong, S. Chao and S. Liu, Dielectric properties and spectroscopy of larger-aspect-ratio ferroelectric thin-film heterostructures, *J. Phys. D: Appl. Phys.* **45**, 335401-1 (2012).
[41]D. K. Kwon and M. H. Lee, Temperature stable high energy density capacitors using complex perovskite thin films, *Applications of Ferroelectrics (ISAF/PFM), 2011 Int. Symp. and 2011 Int. Symp. Piezoresponse Force Microscopy and Nanoscale Phenomena in Polar Mater.* (2011), pp. 1−4.
[42]N. Ortega, A. Kumar, J. F. Scott, D. B. Chrisey, M. Tomazawa, S. Kumari, D. G. B. Diestra and R. S. Katiyar, Relaxor-ferroelectric superlattices: High energy density capacitors, *J. Phys.: Condens. Matter* **24**, 445901-1 (2012).
[43]X. Hao, Y. Wang, J. Yang, S. An and J. Xu, High energy-storage performance in PLZT relaxor ferroelectric thin films, *J. Appl. Phys.* **112**, 114111-1 (2012).
[44]Q. Zhang, L. Wang, J. Luo, Q. Tang and J. Du, Improved energy storage density in barium strontium titanate by Addition of BaO-SiO_2-B_2O_3 glass, *J. Am. Ceram. Soc.* **92**, 1871 (2009).
[45]J. Du, B. Jones and M. Lanagan, Preparation and characterization of dielectric glass-ceramics in Na_2O-PbO-Nb_2O_3-SiO_2 system, *Mater. Lett.* **59**, 2821 (2005).
[46]Q. Zhang, L. Wang, J. Luo, Q. Tang and J. Du, $Ba_{0.4}Sr_{0.6}TiO_3$/MgO composites with enhanced energy storage density and low dielectric loss for solid-state pulse-forming line, *Int. J. Appl. Ceram. Technol.* **7**, E124 (2010).
[47]K. Chen, Y. Pu, N. Xu and X. Luo, Effects of SrO-B_2O_3-SiO_2 glassadditvie on densification and energy storage properties of $Ba_{0.4}Sr_{0.6}TiO_3$ ceramics, *J. Mater. Sci.: Mater. Electron.* **23**, 1599 (2012).
[48]V. S. Puli, D. K. Pradhan, A. Kumar, R. S. Katiyar, X. Su, C. M. Busta, M. Tomozawa and D. B. Chrisey, Structure and dielectric properties of BaO-B_2O_3-ZnO-$[(BaZr_{0.2}Ti_{0.8})O_3]_{0.85}$-$[(Ba_{0.70}Ca_{0.30})TiO_3]_{0.15}$ glass-ceramics for energy storage, *J. Mater. Sci.: Mater. Electron.* **23**, 2005 (2012).
[49]E. P. Gorzkowski, M. J. Pan, B. Bender and C. C. M. Wu, Glass-ceramics of barium strontium titanate for high energy density capacitors, *J. Electroceram.* **18**, 269 (2007).
[50]Y. Zhang, J. Huang, T. Ma, X. Wang, C. Deng and X. Dai, Sintering temperature dependent of energy-storage properties in $(Ba,Sr)TiO_3$ glass-ceramics, *J. Am. Ceram. Soc.* **94**, 1805 (2011).
[51]J. Luo, J. Du, Q. Tang and C. Mao, Lead sodium niobate glass-ceramic dielectrics and internal electrode structure for high energy storage density capacitors, *IEEE Trans. Electron Devices* **55**, 3549 (2008).
[52]J. Luo, Q. Tang, Q. Zhang, L. Wang, J. Du, H. Li and J. Liu, Improved discharge properties of bulk Na_2O-BaO-PbO-Nb_2O_5-SiO_2 glass-ceramic dielectrics through electrode structure design, *Mater. Lett.* **65**, 1976 (2011).
[53]J. Chen, Y. Zhang, C. Deng and X. Dai, Improvement in the microstructures and dielectric properties of barium strontium titanate glass-ceramics by AlF_3/MnO_2 addition, *J. Am. Ceram. Soc.* **92**, 1863 (2009).
[54]X. Wang, Y. Zhang, T. Ma, Z. Yuan, Q. Zhang, C. Deng and T. Liang, Influence of AlF_3 concentration on microstructures and energy storage properties of barium strontium titanate glass ceramics, *Int. J. Appl. Ceram. Technol.*, doi: 10.1111/j.1744-7402.2011.02733.x.
[55]Y. Zhou, Q. Zhang, J. Luo, Q. Tang and J. Du, Structural optimization and improved discharged energy density for niobate glass-ceramics by La_2O_3 addition, *J. Am. Ceram. Soc.*, doi: 10.1111/jace.12159.
[56]D. F. Han, Q. M. Zhang, J. Luo, Q. Tang and J. Du, Optimization of energy storage density in ANb_2O_5-$NaNbO_3$-SiO_2 (A=[(1-x)Pb, xSr] nanastructured glass-ceramic dielectrics, *Ceram. Int.* **38**, 6903 (2012).
[57]Y. Wang, X. Zhou, M. Lin and Q. M. Zhang, High-energy density in aromatic polyurea thin films, *Appl. Phys. Lett.* **94**, 202905-1 (2009).
[58]W. Li, Q. Meng, Y. Zheng, Z. Zhang, W. Xia and Z. Xu, Electric energy storage properties of poly(vinylidene fluride), *Appl. Phys. Lett.* **96**, 192905-1 (2010).
[59]X. Yuan and T. C. M. Chung, Cross-linking effect on dielectric properties of polypropylene thin films and application in electric energy storage, *Appl. Phys. Lett.* **98**, 062901-1 (2011).
[60]S. Wu, W. Li, M. Lin, Q. Burlingame, Q. Chen, A. Payzant, K. Xiao and Q. M. Zhang, Aromatic polythiourea dielectrics with ultrahigh breakdown field strength, low dielectric loss, and high electric energy density, *Adv. Mater.*, doi: 10.1002/adma.201204072.

[61]Y. Wang, X. Zhou, Q. Cheng, B. Chu and Q. Zhang, Recent development of high energy density polymers for dielectric capacitors, *IEEE Trans. Dielectr. Electr. Insul.* **17**, 1036 (2010).
[62]P. Barber, S. Balasubramanian, Y. Anguchamy, S. Gong, A. Wibowo, H. Gao, H. J. Ploehn and H. C. Z. Loye, Polymer composite and nanocomposite dielectric materials for pulse power energy storage, *Materials* **2**, 1697 (2009).
[63]T. C. M. Chung, Functionalization of polypropylene with high dielectric properties: Application in electric energy storage, *Green and Sustain. Chem.* **2**, 29 (2012).
[64]L. Zhu and Q. Wang, Novel ferroelectric polymer for high energy density and low loss dielectrics, *Macromolecules* **45**, 2937 (2012).
[65]L. Zhang and Z.-Y. Cheng, Development of polymer-based 0-3 composites with high dielectric constant, *J. Adv. Dielect.* **1**, 389 (2011).
[66]B. Chu, X. Zhou, K. Ren, B. Neese, M. Liu, Q. Wang, F. Bauer and Q. M. Zhang, A dielectric polymer with high electric energy density and fast discharge speed, *Science* **313**, 334 (2006).
[67]F. Guan, J. Pan, J. Wang, Q. Wang and L. Zhu, Crystal orientation effect on electric energy storage in poly(vinylidene fluride-co-hexafluoropropylene) copolymers, *Macromolecules* **43**, 384 (2010).
[68]W. Xia, X. Xu, F. Wen, W. Li and Z. Zhang, Crystalline properties dependence of dielectric and energy storage properties of poly (vinylidene fluoride-chlorotrifluoroethylene), *Appl. Phys. Lett.* **97**, 222905-1 (2010).
[69]V. Tomer, E. Manias and C. A. Randall, High field properties and energy storage in nanocomposite dielectrics of poly(vinylidene fluoride-hexafluoropropylene), *J. Appl. Phys.* **110**, 044107-1 (2011).
[70]F. Guan, L. Yang, J. Wang, B. Guan, K. Han, Q. Wang and L. Zhu, Confined ferroelectric properties in poly(vinylidene fluoride-co-chlorotrifluoroethylene)-graft-polystyrene graft copolymers for electric energy storage applications, *Adv. Funct. Mater.* **21**, 3176 (2011).
[71]S. Wu, M. Lin, S. G. Lu, L. Zhu and Q. M. Zhang, Polar-fluoropolymer blends with tailored nanostructures for high energy density low loss capacitor applications, *Appl. Phys. Lett.* **99**, 132901-1 (2011).
[72]M. Rahimabady, S. Chen, K. Yao, F. E. H. Tay and L. Lu, High electric breakdown strength and energy density in vinylidene fluoride oligomer/poly(vinylidene fluoride) blend thin films, *Appl. Phys. Lett.* **99**, 142901-1 (2011).
[73]J. Claude, Y. Lu, K. Li and Q. Wang, Electrical storage in poly (vinylidene fluoride) based ferroelectric polymers: Correlating polymer structure to electrical breakdown strength, *Chem. Mater.* **20**, 2078 (2008).
[74]F. Guan, J. Wang, J. Pan, Q. Wang and L. Zhu, Effects of polymorphism and crystallite size on dipole reorientation in poly (vinylidene fluoride) and its random copolymers, *Macromolecules* **43**, 6769 (2010).
[75]F. Guan, J. Wang, L. Yang, J.-K. Tseng, K. Han, Q. Wang and L. Zhu, Confinement-induced high-field antiferroelectric —like behavior in a poly(vinylidene fluoride-co-trifluoroethylene-co-chlorotrifluoroethylene)-graft-polystyrene graft copolymer, *Macromolecules* **44**, 2290 (2011).
[76]X. Zhou, B. Chu, B. Neese, M. Lin and Q. M. Zhang, Electrical energy density and discharge characteristics of a poly(vinylidene fluoride-chlorotrifluoroethylene) copolymer, *IEEE Trans. Dielectr. Electr. Insul.* **14**, 1133 (2007).
[77]F. Guan, J. Wang, L. Zhu, J. Pan and Q. Wang, Effects of films processing condition on electric energy storage for pulsed power application, *IEEE Trans. Dielectr. Electr. Insul.* **18**, 1293 (2011).
[78]Z. Zhang and T. C. M. Chung, The structure-properties relationship of poly(vinylidene difuoride)-based polymers with energy storage and loss under Applied electric fields, *Macromolecules* **40**, 9391 (2007).
[79]Z. Zhang and T. C. M. Chung, Study of VDF/TrEF/CTFE terpolymers for high pulsed capacitors with high energy density and low energy loss, *Macromolecules* **40**, 783 (2007).
[80]Z. Zhang, Q. Meng and T. C. M. Chung, Energy storage study of ferroelectric poly(vinylidene fluoride-trifluoroethylene-chlorotrifluoroethylene) terpolymers, *Polymer* **50**, 707 (2009).
[81]J. Li, S. I. Seok, B. Chu, F. Dogan, Q. Zhang and Q. Wang, Nanocomposites of ferroelectric polymers with TiO_2 nanoparticles exhibiting significantly enhanced electrical enegy density, *Adv. Mater.* **21**, 217 (2009).
[82]P. Kim, S. C. Jones, P. J. Hotchkiss, J. N. Haddock, B. Kippelen, S. R. Marder and J. W. Perry, Phosphnoic acid-modified barium titanate polymer nanocomposites with high permittivity and dielectric strength, *Adv. Mater.* **19**, 1001 (2007).
[83]J. Li, J. Claude, L. E. N. Franco, S. I. Seok and Q. Wang, Electrical energy storage in ferroelectric polymer nanocomposites containing surface-functionalized $BaTiO_3$ nanoparticles, *Chem. Mater.* **20**, 6304 (2008).
[84]H. Tang, Y. Lin, C. Andrews and H. A. Sodano, Nanocomposites with increased energy density through high aspect ratio PZT nanowires, *Nanotechnology* **22**, 015702-1 (2011).
[85]J. Li, P. Khanchaitit, K. Han and Q. Wang, New route toward high-energy-density nanocomposites based on chain-end functionalized ferroelectric polymer, *Chem. Mater.* **22**, 5350 (2010).
[86]S. Lin, X. Kuang, F. Wang and H. Zhu, Effect of TiO_2 crystalline composition on the dielectric properties of TiO_2/P(VDF-TrFE) composites, *Phys. Status Solidi RRL* **6**, 352 (2012).
[87]X. Shan, L. Zhang, X. Yang and Z.-Y. Cheng, Dielectric composites with a high and temperature-independent dielectric constant, *J. Adv. Ceram.* **1**, 310 (2012).
[88]B. Chu, M. Lin, B. Neese, X. Zhou, Q. Chen and Q. M. Zhang, Large enhancement in polarization response and energy density of poly(vinylidene fluoride-trifluoroethylene-chlorofluoroethylene) by interface effect in nanocomposites, *Appl. Phys. Lett.* **91**, 122909-1 (2007).
[89]K. Yu, H. Wang, Y. Zhou, Y. Bai and Y. Niu, Enhanced dielectric properties of $BaTiO_3$/poly(vinylidene fluoride nanocomposites for energy storage applications, *J. Appl. Phys.* **113**, 034105-1(2013).
[90]Y. Song, Y. Shen, P. Hu, Y. Lin, M. Li and C. W. Nan, Significant enhancement in energy density of polymer composites induced by dopamine-modified $Ba_{0.6}Sr_{0.4}TiO_3$ nanofibers, *Appl. Phys. Lett.* **101**, 152904-1 (2012).
[91]Y. Song, Y. Shen, H. Liu, Y. Lin, M. Li and C.-W. Nan, Improving the dielectric constant and breakdown strength of polymer composites: Effects of the shape of the $BaTiO_3$ nanoinclusions, surface modification and polymer matrix, *J. Mater. Chem.* **22**, 16491 (2012).
[92]Y. Song, Y. Shen, H. Liu, Y. Lin, M. Li and C.-W. Nan, Enhanced dielectric and ferroelectric properties induced by dopamine-modified $BaTiO_3$ nanofibers in flexible poly(vinylidene fluoride-trifluoroethylene) nanocomposites, *J. Mater. Chem.* **22**, 8063 (2012).